Influence of spatial incident angles on polarizer with a slit in grooved metal slabs for terahertz communication

MingHui Yuan, Di Zhao, YiBin Zhang, Bin Cai, Lin Chen, and YiMing Zhu*

Shanghai Key Lab of Modern Optical System and Engineering Research Center of Optical Instrument and System, Ministry of Education, University of Shanghai for Science and Technology, No. 516 JunGong Road, Shanghai 200093, China

*Corresponding author: ymzhu@usst.edu.cn

Received 2 September 2014; revised 18 November 2014; accepted 10 January 2015; posted 13 January 2015 (Doc. ID 222357); published 13 February 2015

We report the influence of two spatial incident angles on a terahertz polarizer, which is based on an aluminum slab with a center slit flanked by symmetrically distributed parallel grooves on both sides. Experimental results show that the polarizer shows narrow bandpass filtering effect with a very small divergence angle at normal incidence, which is very suitable for terahertz communication, and the extinction ratio (ER) can be achieved above 20 dB in the frequency band between 0.3 and 0.36 THz due to the excitation of spoof surface plasmon. As the structure rotates around the slit direction (β), the transmission peak will split into two and degrade quickly and the ER decreased down to 20 dB for $\beta = 10°$ at peak position. Rotating along grating period direction (γ) shows better tuning performance. The tuning frequency window can reach from 0.3 to 0.36 THz to promise an ER above 20 dB as γ is smaller than 25°.

OCIS codes: (230.5440) Polarization-selective devices; (240.5440) Polarization-selective devices.
http://dx.doi.org/10.1364/AO.54.001363

1. Introduction

Terahertz (THz) wave has been a research highlight during the past decades, because of its potential applications in sensing, imaging, spectroscopy, and communications [1]. With the rapid progress of terahertz technology, the demands for high-performance devices, such as narrowband filters, switches and polarizers, are increasing. THz polarizers can also be used to characterize the electric field distribution of THz antennae or remove unwanted components [2,3]. A polarizer with low cost and high efficiency is critical for polarizing THz waves. Generally speaking, wire grid type [4,5] and liquid crystal [6] based elements are widely used to design and fabricate THz polarizers. Extraordinary optical transmission (EOT) effect has also been used for polarizer design in metallic structures (such as a wire grid) [7,8]. More recently, novel THz carbon nanotube layer polarizers have been reported [9,10] due to the good polarized performances of carbon nanotube, but the fabrication cost for carbon nanotubes is a huge challenge.

The slit-groove array structures with a given number of grooves that are symmetrically distributed with respect to a central slit had been widely studied in the visible range owing to their EOT at a narrow spectral range [11,12]. The physical mechanism of EOT in the visible range is the resonant coupling of electromagnetic radiation with surface plasmons (SPs) on the metal surface. However, in the THz region, the mechanism for EOT is not SP coupling because metal conductors show much larger real and imaginary parts of the complex permittivity in the THz frequency, resulting in delocalization of SPs. According to Pentry's theory [13], the incident THz wave is coupled into spoof surface plasmon polariton (SPP) mode and propagated through in the structured surfaces of both sides so that our proposed structure has a very high center transmittance. So such structures are always thought to have potential application for resonant narrow bandpass filter [14]. It is

1559-128X/15/061363-06$15.00/0

worth noting that the terahertz transmission of a single slit in a thin metallic structure shows the polarization-dependent property, which can be used to design a novel THz polarizer [15]. However, the design of a THz polarizer based on this principle has not been fully studied. In addition, further studies on different types of polarizers for terahertz communication are still needed [16]. Therefore, it is valuable to investigate the novel design of a polarizer in the THz range. In this paper, we present the design and analysis of a THz polarizer based on a narrow slit in corrugated aluminum slabs theoretically and experimentally. Compared to the structure in Ref. [15], our proposed structure has a center slit flanked by symmetrically distributed parallel grooves on both sides to further enhance the spoof SP effect. The proposed polarizer has the performance of extinction ratio (ER) above 20 dB in the frequency band between 0.3 and 0.36 THz, which is larger than 11.4 GHz proposed in Ref. [16]. Moreover, we show that its performance accommodates reasonable tolerances of spatial incident angles. Rotating γ shows better tuning performance in our structure.

2. Experimental Results and Analysis

Stereogram and profile of the proposed THz polarizer are shown in Figs. 1(a) and 1(b), respectively. The periodical structure at the interface behaves like an antenna which collects and couples the incident wave into spoof SP at a special incident wavelength λ, which is decided by the groove period p, resulting in very intensive fields near the aperture. The optimal values are analyzed numerically prior to this paper by the finite element method and the parameters of the structure ($d/p = 0.25$, $w/p = 0.5$, and $s/t = 0.2$) are the optimized results to achieve optimal transmission characteristics of the THz wave through the structure [17]. The SEM image is shown in Fig. 1(c). To identify the angles α, β, and γ in Fig. 1(d) we use blue, green, and red lines to mark the axes x, y, and z. We note that the polariton angle α is in the plane xy; the angle β, which is the angle between the incident wave and the principal axis x, is in the plane xz; the angle γ, which is the angle between the incident wave and the principal axis y, is in the plane yz. The transmission properties are tested by the THz time domain spectroscopy (THz-TDS) system [18–21].

First, for comparison, we studied the "pass" state of polarizer at normal and perpendicular (TM) polarized ($\alpha = 0°$) incidence. The measured transmitted THz waveform and corresponding relative amplitude are shown in Figs. 2(a) and 2(b), respectively. A high center transmittance (>95%) at 0.33 THz is experimentally observed due to the enhancement effect between symmetrically coupled spoof SP in both sides of the slab. According to the quasi-momentum conservation rule [14]:

$$\kappa_{\parallel} + \kappa_{\mathrm{spp}} = G^{(i)}, \tag{1}$$

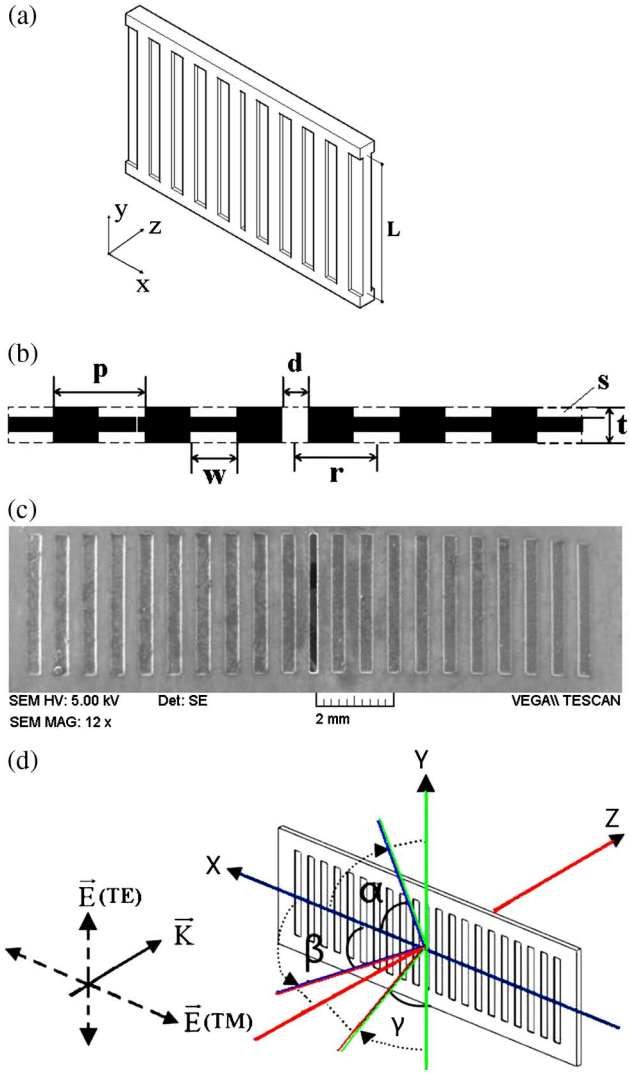

Fig. 1. Notation used for describing a narrow slit in corrugated aluminum slabs [(a) stereogram and (b) profile]. It consists of an aluminum slab with thickness $t = 300$ μm. The slab is structured by $2 \times 10 \times 2$ parallel grooves with length $L = 4400$ μm, width $w = 440$ μm, depth $s = 60$ μm, separated by a period $p = 880$ μm on both sides. A single slit with width $d = 220$ μm is milled through the slab at a distance of $r = 770$ μm from the center to the first groove. (c) Scanning electronic microscopy (SEM) image and (d) rotation schematic graph.

where $\kappa_{\parallel}$ is the wave vector parallel to the x axis, $\kappa_{\mathrm{spp}} = (2\pi f/c) \times (\varepsilon_{\mathrm{Al}}\varepsilon_{\mathrm{air}}/(\varepsilon_{\mathrm{Al}} + \varepsilon_{\mathrm{air}}))^{1/2}$ is the wavenumber of spoof SP, and $G^{(i)} = 2\pi i/p$ ($i \in N$) is the periodical corrugation momentum. The permittivity of Al at around 1 THz is about $\varepsilon_{\mathrm{Al}} = -44900 + j511000$ [14], which is much larger than that in the visible range [22]. Therefore, we can approximate $(\varepsilon_{\mathrm{Al}}\varepsilon_{\mathrm{air}}/(\varepsilon_{\mathrm{Al}} + \varepsilon_{\mathrm{air}}))^{1/2} \approx 1$. From Eq. (1), we can get the main ($i = 1$) resonant frequency f_0 at normal incidence is 0.34 THz, which agrees well with the measured value.

Next, we discuss the ER of this polarizer by rotating polarization angle α. Figures 3(a) and 3(b) show transmitted THz waveforms and corresponding transmission spectra as a function of polarization

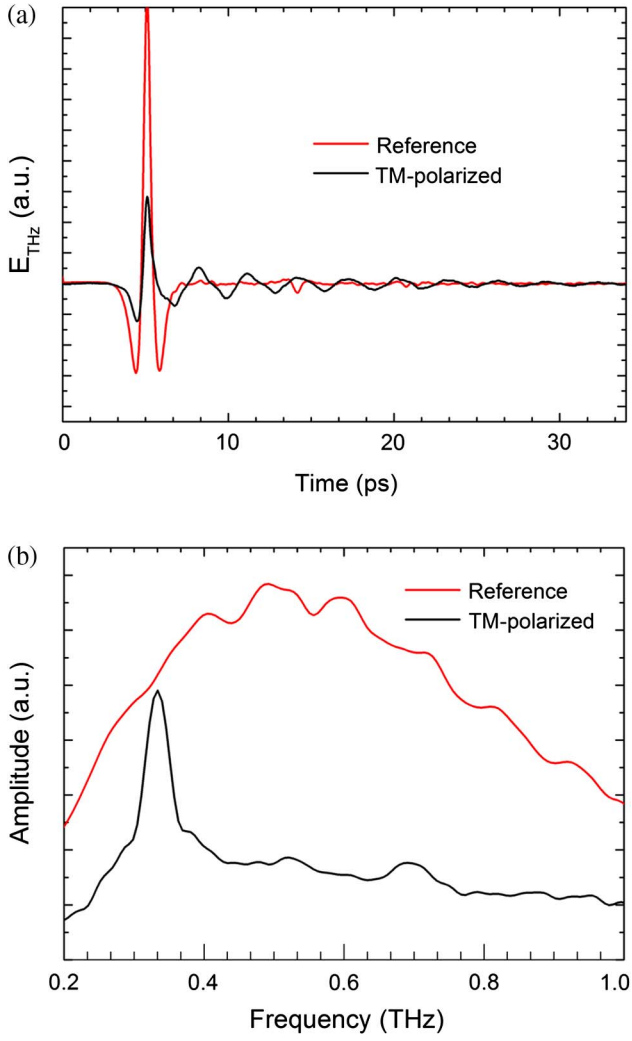

Fig. 2. (a) Transmitted THz waveform and (b) corresponding transmission spectra at normal incidence.

angle α, respectively. Because the periodical corrugation momentum G is directional (along the x axis) and only the TM-polarized component can be coupled into spoof SP mode, the transmittance decreases when the polarization angle α increases. The ER is defined as $-10\log(T_{TM}/T_{TE})$, where T_{TM} and T_{TE} are the transmittances of TM($\alpha = 0$) and TE($\alpha = 90°$) polarized waves, respectively [8]. An ER of 28.2 dB at 0.33 THz is measured and the ER varies from 20.0 to 28.2 dB at 0.3–0.36 THz, as shown in Fig. 4. This polarizer has a bandwidth of about 60 GHz at normal incidence. The transmission peak of the polarizer is a good property, especially for detecting signals around the resonant frequency 0.33 THz in communication application.

3. Influence of Spatial Incident Angles on the Polarizer Performance

In this section, we demonstrate the influence of two spatial incident angles on the frequency band and ER of the polarizer. In the first case, we discuss the incident angle β between the wave vector and the x axis

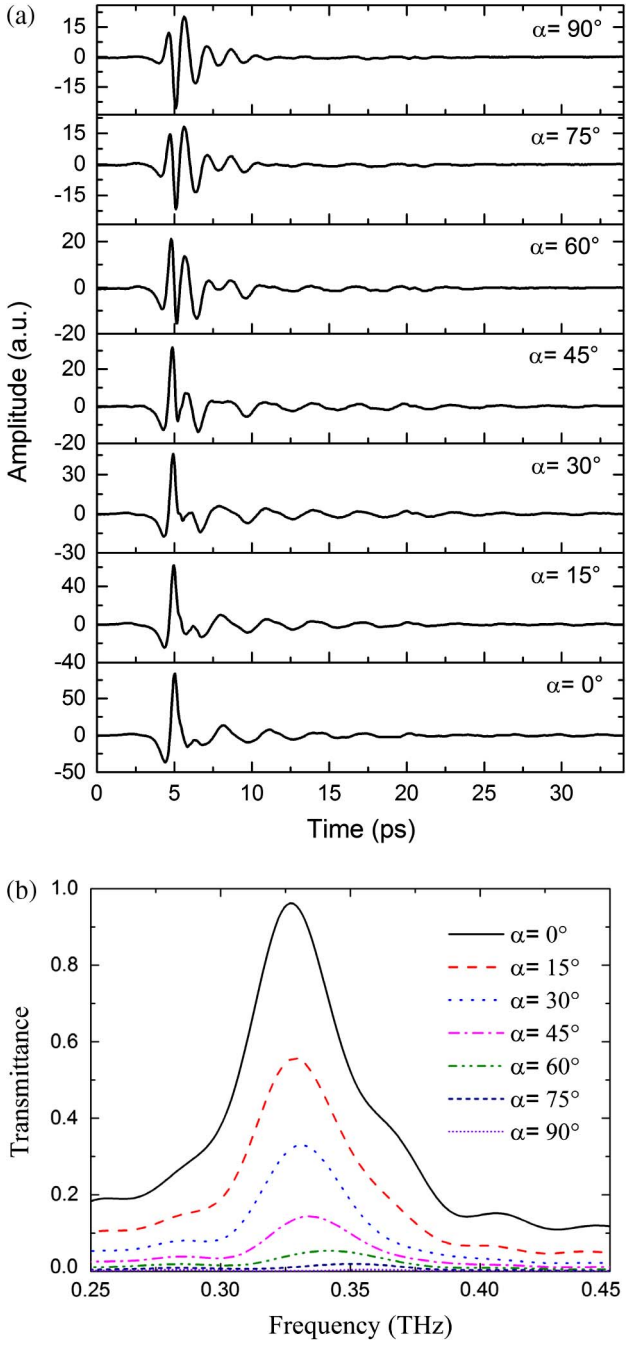

Fig. 3. (a) Transmitted THz waveforms and (b) corresponding transmission spectra as a function of polarization angle α from pass state ($\alpha = 0°$, TM polarization) to rejection state ($\alpha = 90°$, TE polarization) with a step of 15°.

[see Fig. 1(d)]. Transmitted TM-polarized THz waveforms, corresponding transmission spectra with different β, are shown in Figs. 5(a) and 5(b), respectively. When β increases, the transmission peak splits into two peaks: the left peak shows redshift and the right peak shows blueshift. The splitting and shifts are induced by the momentum matching condition, where the periodical corrugation momentums of grooves on two sides of the slit and $\kappa_{||}$ are with the same and reverse directions, respectively.

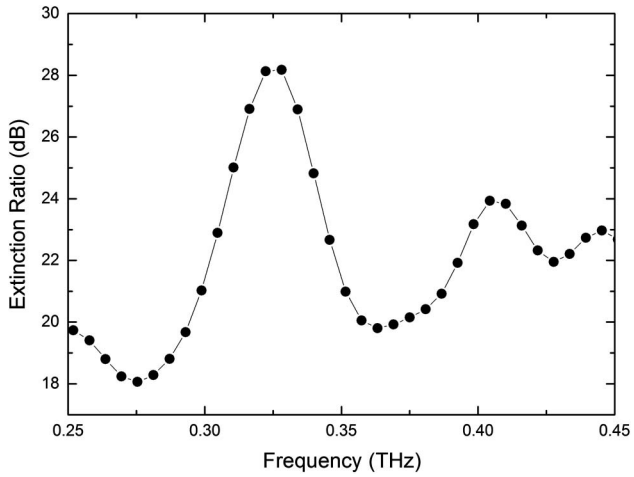

Fig. 4. Extinction Ratio versus frequency.

According to Eq. (1), the main resonant frequency f_β can be expressed as $f_0/(1+\sin\beta)$. The calculated results agree with the measured values in Fig. 5(c). In addition, it is not practical to tune the center frequency by rotating the angle β because the transmission peak will degrade quickly. The dependence of the transmission peak on angle β has been shown in Fig. 5(d). But we can evaluate the performance influence by rotating angle β. Experimental results show that the ER decreased down to 20 dB for $\beta = 10°$.

In the second case, we focused on the incident pitching angle γ. Transmitted TM-polarized THz waveforms and corresponding transmission spectra as a function of γ are shown in Figs. 6(a) and 6(b). Unlike the first case, the transmission peak blueshifts and broadens when γ increases. This is because the incident wave component in y direction [as shown in Fig. 1(d)] cannot be coupled to spoof SP mode. Similarly, the resonant frequency f_γ is given by $f_0/\cos\gamma$. The calculated results shown in Fig. 6(c) fit well with the measured values. Here, we note that rotating angle γ shows better tuning performance. Figure 6(d) shows the peak transmittance and full width at half-maximum (FWHM) as the function of angle γ. We can see that the peak transmittance decreases and FWHM increases as increase of angle γ. For example, the transmittance declines to about 0.55 as $\gamma = 30°$, at the same time FWHM broadens only from 37 to 63 GHz. To clearly understand how angle γ can affect the performance of this structure, Fig. 6(e) shows the ER (dB) versus angle γ for 0.3, 0.33, and 0.36 THz. At normal incidence the ER of above 20 dB can be achieved for frequency range between 0.3 and 0.36 THz. From Fig. 6(e) we can also see that at 0.3 THz the ER remains above 20 dB as γ is smaller than 25°. At 0.36 THz the ER increases with increasing γ up to a peak of about 24 dB at $\gamma = 20°$. Beyond this peak the ER drops precipitously. This makes sense physically because the center frequency corresponding to the transmittance peak show blueshift with increasing γ. When γ is equal to 20° the center frequency corresponding to the

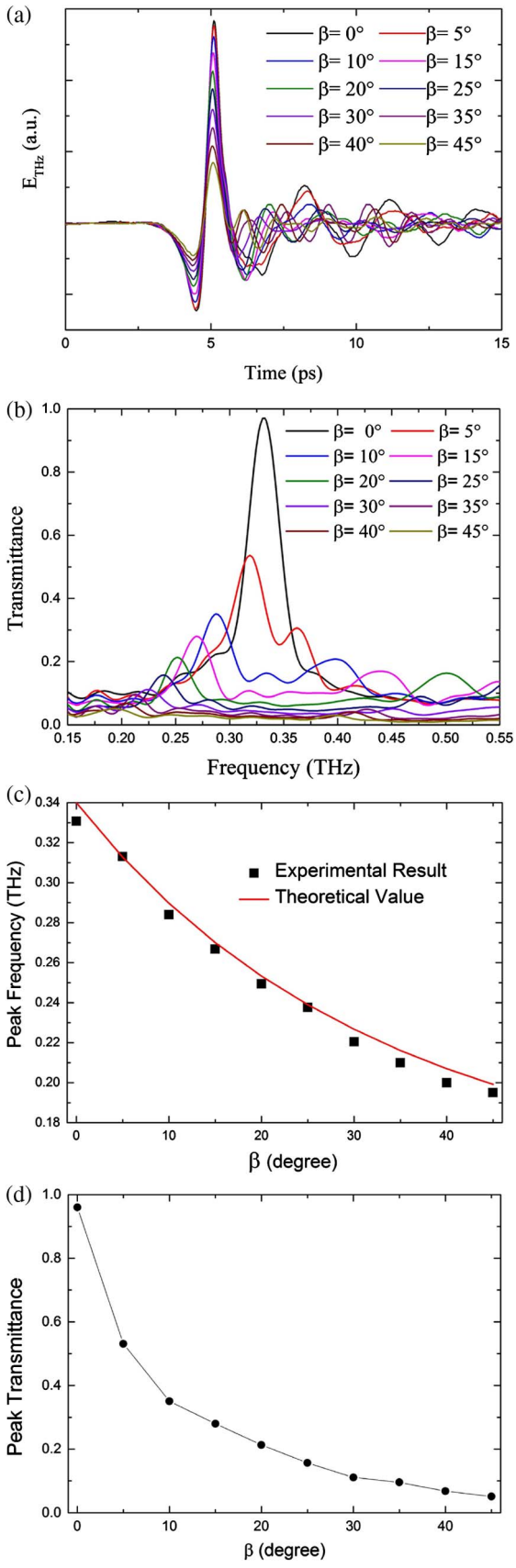

Fig. 5. (a) Transmitted THz waveforms, (b) corresponding transmission spectra, (c) main (left) resonant frequencies, and (d) main (left) peak transmittance as a function of angle β from 0° to 45° with a step of 5°.

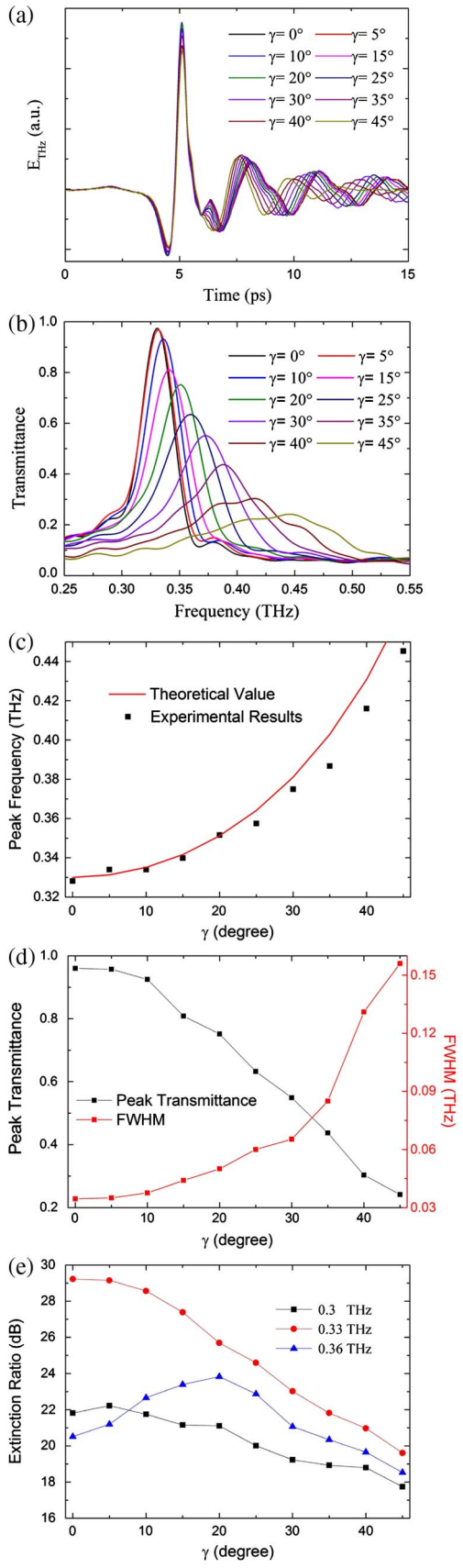

Fig. 6. (a) Transmitted THz waveforms, (b) corresponding transmission spectra, (c) peak frequencies, and (d) peak transmittance and FWHM as a function of incident pitching angle γ from 0° to 45° with a step of 5°. (e) ER versus angle γ for 0.3, 0.33, and 0.36 THz.

transmittance peak just exactly locates at 0.36 THz, leading to the high ER. At 0.33 THz the ER is larger than that at 0.3 THz and 0.36 THz. Here we can find that as γ is smaller than 25°, the tuning frequency window can reach from 0.3 to 0.36 THz to promise the ER above 20 dB.

4. Conclusion

The transmittance properties of a THz polarizer based on an aluminum slab with a center slit flanked by symmetrically distributed parallel grooves on both sides are experimentally investigated by using THz-TDS. For the frequency range between 0.3 and 0.36 THz, the polarizer is highly transmitting with a very small divergence angle for TM polarization and the ER can reach above 24 dB. It also shows that the transmission band frequency has a redshift (blueshift) as the spatial incidence angle β (incident pitch angle γ) is increasing. The present polarizer is angle-flexible and could be used for the generation and detection of arbitrarily polarized THz radiation. Potential applications, such as communications, imaging, and sensing, would be pursued.

This work was partly supported by the National Program on Key Basic Research Project of China (973 Program, 2014CB339806), National Natural Science Foundation of China (11174207, 61138001, 61205094, and 61307126), Major National Development Project of Scientific Instrument and Equipment (2011YQ150021 and 2012YQ14000504), the Key Scientific and Technological Project of Shanghai Municipality (12142200100), Shanghai Rising-Star Program (14QA1403100), Program of Shanghai Subject Chief Scientist (14XD1403000), Basic Research Key Project (12JC1407100), and Science Foundation of Shanghai (11ZR1424900).

References

1. M. Tonouchi, "Cutting-edge terahertz technology," Nat. Photonics **1**, 97–105 (2007).
2. M. Reid, I. Cravetchi, and R. Fedosejevs, "Terahertz radiation and second-harmonic generation from InAs: bulk versus surface electric-field-induced contributions," Phys. Rev. B **72**, 035201 (2005).
3. Y. Cai, I. Brener, J. Lopata, J. Wynn, L. Pfeiffer, and J. Federici, "Design and performance of singular electric field terahertz photoconducting antennas," Appl. Phys. Lett. **71**, 2076–2078 (1997).
4. Z. Huang, H. Park, E. Parrott, H. P. Chan, and E. P. MacPherson, "Robust thin-film wire-grid THz polarizer fabricated via a low-cost approach," IEEE Photon. Technol. Lett. **25**, 81–84 (2013).
5. A. Wojdyla and G. Gallot, "Brewster's angle silicon wafer terahertz linear polarizer," Opt. Express **19**, 14099–14107 (2011).
6. C. F. Hsieh, Y. C. Lai, R. P. Pan, and C. L. Pan, "Polarizing terahertz waves with nematic liquid crystals," Opt. Lett. **33**, 1174–1176 (2008).
7. I. Yamada, K. Takano, M. Hangyo, M. Saito, and W. Watanabe, "Terahertz wire-grid polarizers with micrometer-pitch Al gratings," Opt. Lett. **34**, 274–276 (2009).
8. J. S. Cetnar, J. R. Middendorf, and E. R. Brown, "Extraordinary optical transmission and extinction in a terahertz wire-grid polarizer," Appl. Phys. Lett. **100**, 231912 (2012).
9. L. Ren, C. L. Pint, T. Arikawa, K. Takeya, I. Kawayama, M. Tonouchi, R. H. Hauge, and J. Kono, "Broadband terahertz

polarizers with ideal performance based on aligned carbon nanotube stacks," Nano Lett. **12**, 787–790 (2012).
10. J. Kyoung, E. Y. Jang, M. R. D. Lima, H. R. Park, R. O. Robles, X. Lepro, Y. H. Kim, R. H. Baughman, and D. S. Kim, "A reel-wound carbon nanotube polarizer for terahertz frequencies," Nano Lett. **11**, 4227–4231 (2011).
11. L. Martin-Moreno, F. J. Garcia-Vidal, H. J. Lezec, A. Degiron, and T. W. Ebbesen, "Theory of highly directional emission from a single subwavelength aperture surrounded by surface corrugations," Phys. Rev. Lett. **90**, 167401 (2003).
12. F. Villate-Guio, F. Lopez-Tejeira, F. J. Garcia-Vidal, L. Martin-Moreno, and F. de Leon-Perez, "Optimal light harvesting structures at optical and infrared frequencies," Opt. Express **20**, 25441–25453 (2012).
13. J. B. Pendry, L. Martin-Moreno, and F. J. Garcia-Vidal, "Mimicking surface plasmons with structured surfaces," Science **305**, 847–848 (2004).
14. L. Chen, Y. M. Zhu, X. F. Zang, B. Cai, Z. Li, L. Xie, and S. L. Zhuang, "Mode splitting transmission effect of surface wave excitation through a metal hole array," Light Sci. Appl. **2**, e60 (2013).
15. J. W. Lee, T. H. Park, P. Nordlander, and D. M. Mittleman, "Terahertz transmission properties of an individual slit in a thin metallic plate," Opt. Express **17**, 12660–12667 (2009).
16. J. S. Li, "A novel terahertz wave reflective polarizer for THz communication," Opt. Commun. **284**, 957–960 (2011).
17. M. H. Yuan, X. Huang, and X. F. Zhang, "Optimization of slit structures for transmission enhancement of THz wave," Microw. Opt. Technol. Lett. **55**, 559–561 (2013).
18. L. Chen, C. M. Gao, J. M. Xu, X. F. Zang, B. Cai, and Y. M. Zhu, "Observation of electromagnetically induced transparency-like transmission in terahertz asymmetric waveguide-cavities systems," Opt. Lett. **38**, 1379–1381 (2013).
19. L. Chen, J. M. Xu, C. M. Gao, X. F. Zang, B. Cai, and Y. M. Zhu, "Manipulating terahertz electromagnetic induced transparency through parallel plate waveguide cavities," Appl. Phys. Lett. **103**, 251105 (2013).
20. L. Chen, Z. Cheng, J. Xu, X. Zang, B. Cai, and Y. Zhu, "Controllable multiband terahertz notch filter based on a parallel plate waveguide with a single deep groove," Opt. Lett. **39**, 4541–4544 (2014).
21. L. Chen, K. V. Truong, Z. X. Cheng, Z. Li, and Y. M. Zhu, "Characterization of photonic bands in metal photonic crystal slabs," Opt. Commun. **333**, 232–236 (2014).
22. L. Chen, Z. Q. Cao, F. Ou, H. G. Li, Q. S. Shen, and H. C. Qiao, "Observation of large positive and negative lateral shifts of a reflected beam from symmetrical metal-cladding waveguides," Opt. Lett. **32**, 1432–1434 (2007).